

# Satellite Data Simulator Unit

## A Multisensor, Multispectral Satellite Simulator Package

BY HIROHIKO MASUNAGA, TOSHIHISA MATSUI, WEI-KUO TAO, ARTHUR Y. HOU, CHRISTIAN D. KUMMEROW, TERUYUKI NAKAJIMA, PETER BAUER, WILLIAM S. OLSON, MIHO SEKIGUCHI, AND TAKASHI Y. NAKAJIMA

Since the earliest meteorological satellites were sent into orbit in the 1960s, satellite remote sensing has been the vital means to monitor clouds and precipitation uniformly across the Earth. Present-day spaceborne remote sensors have great variety in terms of spectral range (visible, infrared, and microwave) and measuring principle (active and passive), each of which has its own strengths and limitations. Satellite imagers equipped with visible and infrared channels are an optimal instrument for deriving cloud-top height and optical thickness, while microwave radiometry is sensitive to the whole cloud column, providing more of a physical link to the underlying rainfall structure. Microwave radiometers, however, typically have a spatial resolution as low as 50 km at the lowest microwave frequencies (e.g., 6 and 10 GHz) and do not resolve the vertical structure of atmospheric constituents. Two spaceborne radars—the TRMM PR and CloudSat CPR (expansions of all acronyms are listed at the end of the article)—launched within the last decade literally added a new dimension to cloud

and precipitation measurements from space. The increasing variety of satellite sensors has greatly expanded the applicability of satellite data, particularly when different sensors are combined to exploit the information content beyond the capability of an individual sensor. Multisensor data analyses vastly enrich the quality (and quantity) of data to be processed, requiring sophisticated analysis software that helps us interpret the observations. Potentially useful for this purpose is a multisensor satellite simulator, or a computer program to derive synthetic measurements for various satellite instruments computed with given meteorological parameters virtually representing the atmospheric and ground state.

Several multisensor simulator packages are being developed by different research groups across the world. Such simulator packages [e.g., COSP (<http://cfmip.metoffice.com/COSP.html>), CRTM ([www.star.nesdis.noaa.gov/smcd/spb/CRTM](http://www.star.nesdis.noaa.gov/smcd/spb/CRTM)), ECSIM (Voors et al. 2007), RTTOV (Matricardi et al. 2004; Bauer et al. 2006), ISSARS (under development, Tanelli 2009), and SDSU (this article), among others] share overall aims, although some are targeted more on particular satellite programs or specific applications (for research purposes or for operational use) than others. The SDSU or Satellite Data Simulator Unit is a general-purpose simulator composed of Fortran 90 codes and applicable to spaceborne microwave radiometer, radar, and visible/infrared imagers including, but not limited to, the sensors listed in Table 1. Table 1 shows satellite programs particularly suitable for multisensor data analysis: some are single satellite missions carrying two or more instruments, while others are constellations of satellites flying in formation. The TRMM and A-Train are ongoing satellite missions carrying diverse sensors that observe clouds and precipitation, and will be continued or augmented within the decade to come by future multisensor missions such as the GPM and Earth-CARE. The ultimate goals of these present and proposed satellite programs are not restricted to clouds

**AFFILIATIONS:** MASUNAGA—Hydrospheric Atmospheric Research Center, Nagoya University, Nagoya, Japan; MATSUI, TAO, HOU, AND OLSON—NASA Goddard Space Flight Center, Greenbelt, Maryland; KUMMEROW—Department of Atmospheric Science, Colorado State University, Fort Collins, Colorado; TE. NAKAJIMA—Atmosphere and Ocean Research Institute, University of Tokyo, Chiba, Japan; BAUER—European Centre for Medium-Range Weather Forecasts, Reading, United Kingdom; SEKIGUCHI—Faculty of Marine Technology, Tokyo University of Marine Science and Technology, Tokyo, Japan; TA. Y. NAKAJIMA—Research and Information Center, Tokai University, Tokyo, Japan  
**CORRESPONDING AUTHOR:** Hirohiko Masunaga, Hydrospheric Atmospheric Research Center, Nagoya University, F3-1(200) Furocho Chikusa-ku, Nagoya 464-8601, Japan  
E-mail: [masunaga@hyarc.nagoya-u.ac.jp](mailto:masunaga@hyarc.nagoya-u.ac.jp)

DOI:10.1175/2010BAMS2809.1

In final form 30 April 2010  
©2010 American Meteorological Society

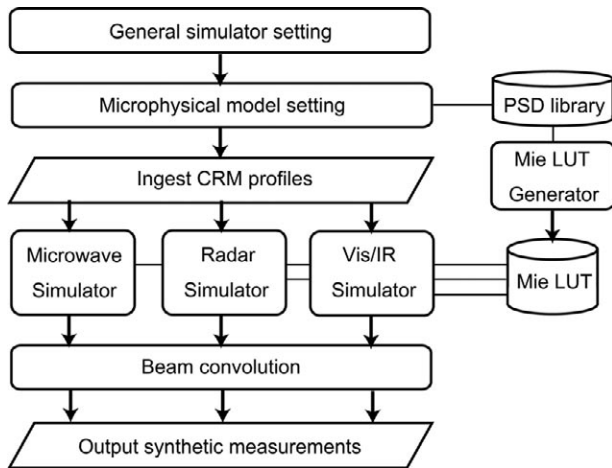


**FIG. 1. SDSU flowchart.**

and precipitation but are to better understand their interactions with atmospheric dynamics/chemistry and feedback to climate. The SDSU’s applicability is not technically limited to hydrometeor measurements either, but may be extended to air temperature and humidity observations by tuning the SDSU to sounding channels. As such, the SDSU and other multisensor simulators would potentially contribute to a broad area of climate and atmospheric sciences.

The SDSU is not optimized to any particular orbital geometry of satellites. The SDSU is applicable not only to low-Earth orbiting platforms as listed in Table 1, but also to geostationary meteorological satellites. Although no geosynchronous satellite carries microwave instruments at present or in the near future, the SDSU would be useful for future geostationary satellites with a microwave radiometer and/or a radar aboard, which could become more feasible as engineering challenges are met.

In this short article, the SDSU algorithm architecture and potential applications are reviewed in brief.

**SDSU STRUCTURE.** Figure 1 outlines the SDSU algorithm flow. General simulator settings including sensor specifications such as channel frequencies/wavelengths are defined first by the user, followed by the microphysical model setting where the particle size distribution (PSD) models are customized using the PSD library (see below). Input meteorological

parameters (e.g., snapshots from a CRM simulation containing temperature, humidity, and hydrometeor profiles) are then ingested and passed on to individual simulator components. As such, the I/O routines and each simulator are designed to be strictly modular so that the user can flexibly customize the SDSU (e.g., modify the I/O interface in a way compatible with the user-provided input data format and/or add a new simulator component to expand the SDSU capability). Technical details about each simulator component are documented in the papers cited in Table 1 and in the SDSU User’s Guide. Antenna pattern convolution is applied to the simulator outputs—that is, simulated synthetic measurements are made “out of focus” so the spatial resolution matches the field of view (FOV) of satellite sensors.

The PSD library is a feature unique to the SDSU that allows the user to set arbitrary PSD models for individual hydrometeor species, facilitating the flexible implementation of various bulk microphysical schemes in radiative transfer calculations. As discussed later, remote-sensing measurements are often

**TABLE 1. SDSU components and applicable multisensor satellite missions.**

Simulator	Microwave radiometer	Radar	Visible/IR imager
<i>Numerical scheme</i>	Kummerow (1993)	Masunaga and Kummerow (2005)	Nakajima et al. (2003)
<i>Missions/sensors applicable</i>			
TRMM	TMI	PR	VIRS
A-Train	Aqua AMSR-E	Cloudsat CPR	Aqua MODIS
GPM	GMI	DPR	
EarthCARE		CPR	MSI

sensitive to the microphysical properties of clouds and precipitation such as, for example, hydrometeor particle size. The SDSU PSD library offers templates of typical PSD functions such as a single- and double-moment exponential and gamma distributions for users’ convenience. The users can either choose from these template PSDs or create their own PSDs and add them to the library. Given the PSD specified by the user, the radiative properties of hydrometeors are computed assuming that all particles are spherical. In a future version of the SDSU, a more sophisticated radiative transfer model will be implemented in which the nonsphericity of hydrometeors is taken into account.

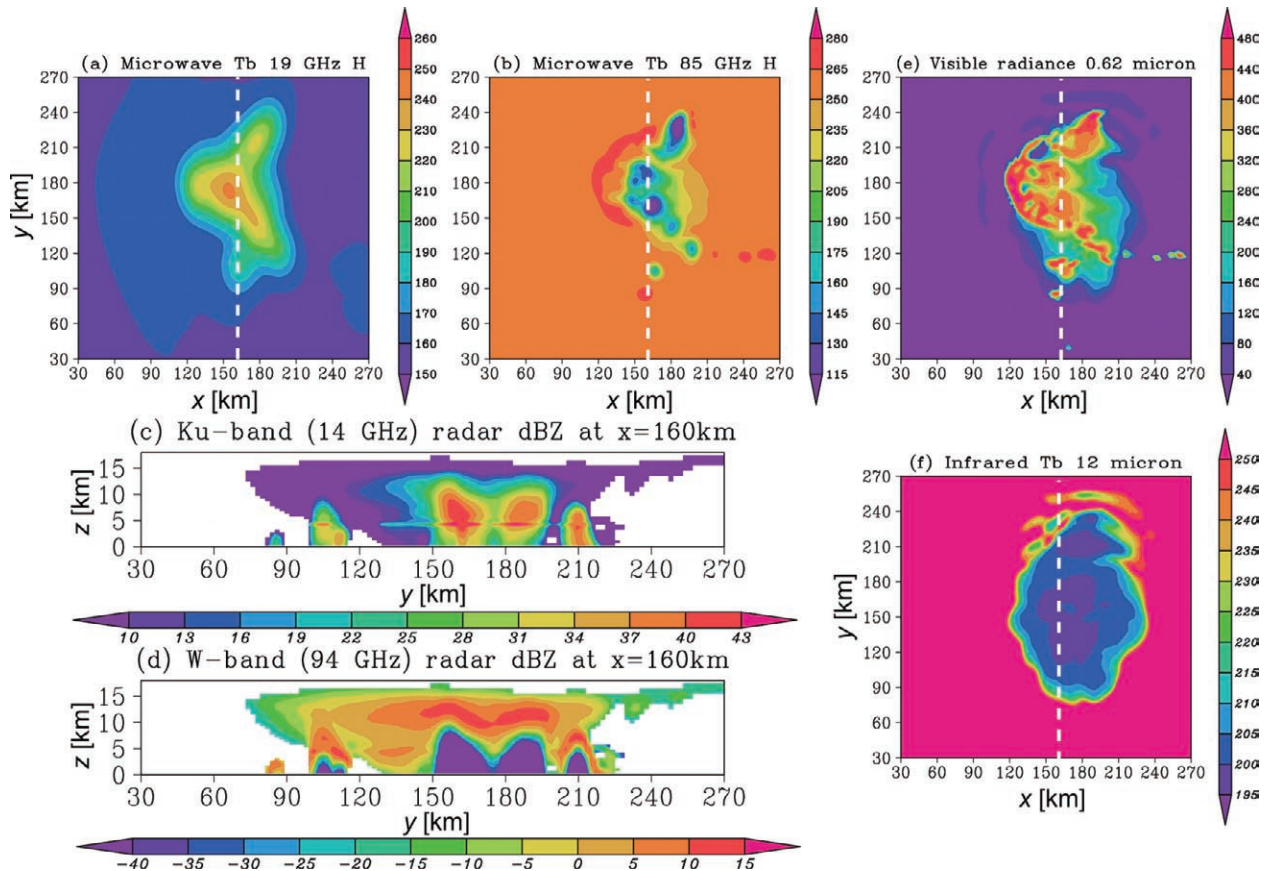


**FIG. 2. Synthetic observations computed with the SDSU, applied to a snapshot of a GCE-simulated tropical squall line. (a) Plan view of 19-GHz microwave brightness temperature [K] in horizontal polarization. Dashed line indicates  $x = 160$  km where the radar cross-section shown in (c) and (d) is sampled. (b) Same as (a) but for 85 GHz. (c) Vertical cross section of 14-GHz radar reflectivity (dBZ) sliced along the  $y$  axis at  $x = 160$  km. (d) Same as (c) but for 94 GHz. (e) Plan view of visible ( $0.62 \mu\text{m}$ ) radiance ( $\text{W m}^{-2} \mu\text{m}^{-1} \text{str}^{-1}$ ). (f) Plan view of thermal infrared ( $12 \mu\text{m}$ ) brightness temperature (K).**

A lookup table (LUT) generator creates precomputed tables of the hydrometeor radiative properties, hereafter called the Mie LUTs. The simulator works several times (or even an order of magnitude) faster when the radiative properties are calculated offline in advance and stored in LUTs so that the simulator quickly refers to the LUTs without repeating time-consuming computations. Since the hydrometeor radiative properties depend on microphysics, the Mie LUT generator is designed to be directly linked with the PSD library when it is compiled for execution.

These features make the SDSU unique compared to conventional satellite simulators used by spacecraft designers and manufacturers. While these simulators are well specialized for testing engineering details of instruments, the SDSU is targeted more on meteorological applications and is flexibly tunable to

realistic atmospheric and surface models. Examples of synthetic satellite measurements simulated with the SDSU are presented in the next section.

### SYNTHETIC SATELLITE OBSERVATIONS.

The SDSU is applied to a CRM-generated mesoscale convective system to illustrate how they would be observed if the TRMM satellite flew over the scene. The example shown in Fig. 2 is a mature tropical squall line simulated by the GCE model and virtually observed by the three primary TRMM sensors: TMI, PR, and VIRS (see Table 1). Synthetic microwave brightness temperature at a low frequency of 19 GHz (Fig. 2a) shows thermal emission from liquid clouds and rainfall that form the main body of the convective system. Deep convective cores are identified as brightness temperature depressions in the map of high-frequency



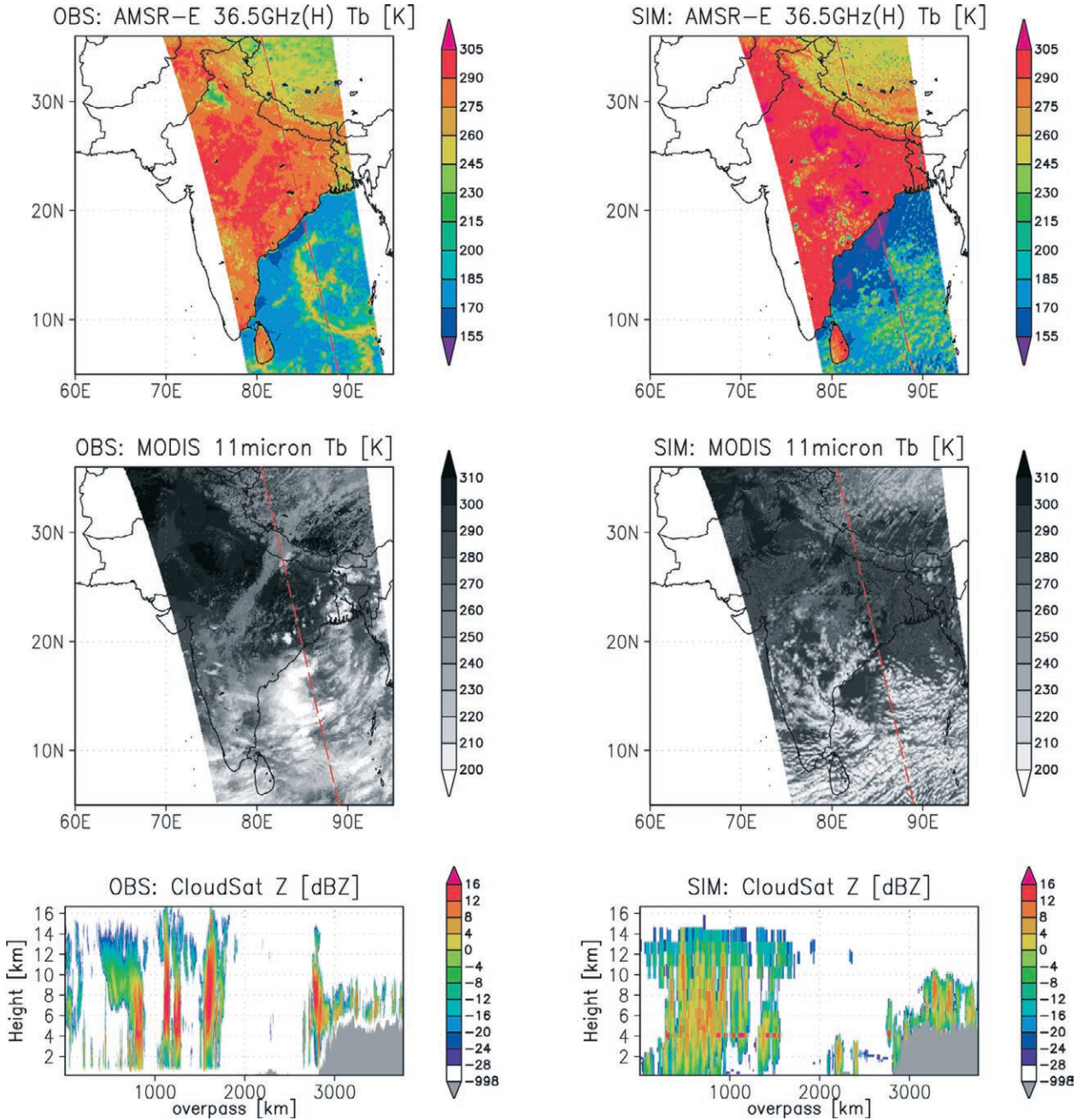


**FIG. 3. (left column) A-Train multisensor observations and (right column) synthetic measurements computed with the Goddard SDSU applied to a WRF simulation. The time stamp is approximately 0750 UTC, 20 Jun 2006. (Top) AMSR-E 36.5-GHz brightness temperature (K); (middle) MODIS 11- $\mu$ m brightness temperature (K); and (bottom) CloudSat radar reflectivity (dBZ). Red, dashed line crossing the top and middle panels indicates the CloudSat overpass.**

(85 GHz) microwave brightness temperature, resulting from microwave scattering by frozen precipitating particles (Fig. 2b). The spatial distribution of brightness temperatures is smoother at 19 GHz than at 85 GHz, as the antenna pattern convolution works more aggres-

sively at lower frequencies (note that the radiometer FOV size is inversely proportional to the channel frequency when observed with the same antenna).

Shown in Fig. 2c is the vertical cross section of simulated TRMM PR (14 GHz) reflectivity in a vertical

plane at  $x = 160$  km. Some of the deep convective cores identified by 85-GHz scattering signals are clearly captured as areas with distinctly large PR echoes. The SDSU, with a simple melting-particle model installed, is able to reproduce the radar bright band, observed around the height of 4 km. For comparison, CloudSat (94 GHz) radar reflectivity is simulated with the same snapshot (Fig. 2d). This frequency is sufficiently high to thoroughly map nonprecipitating cloud decks extending into the upper troposphere, whereas lower portions of deep convective cores are left undetected as a result of the severe attenuation of radar echo by the thick layer of condensate above.

While microwave radiometry is a rough proxy for the total liquid and ice water constituted of millimeter-size precipitation particles, visible imagery is sensitive to smaller cloud droplets that may or may not accompany precipitation. When observed in the visible (Fig. 2e), the convective system in this particular case exhibits a complicated texture, including a line of shallow clouds newly spawned along a bow-shaped convective leading edge. Infrared brightness temperatures (Fig. 2f) delineate the cloud-top temperature, nearly as cold as 200 K, of extensive high clouds spreading entirely over the convective system. A series of synthetic observations shown by Fig. 2 implies that the three TRMM instruments provide different pieces of complementary information, and that a thorough picture of the convective system emerges only when observations from all the sensors are combined together.

Another example of synthetic measurements is presented in Fig. 3 together with corresponding observations by the AMSR-E, MODIS, and CloudSat. In this particular case, the A-Train constellation follows a track from the Bay of Bengal to the Tibetan plateau at roughly 0750 UTC on 20 June 2006. For the input model, a WRF simulation forced by the NCEP Global Forecast System was run with the GCE one-moment bulk microphysics and Goddard radiation schemes. Synthetic measurements of AMSR-E 36.5-GHz brightness temperature, MODIS 11- $\mu\text{m}$  brightness temperature, and CloudSat radar reflectivity were computed using the Goddard SDSU (see the last section of this article for a description). A tropical disturbance observed by the AMSR-E and MODIS over the Bay of Bengal is generally captured by the WRF simulation, although the disturbance consists of numerous cloud cells scattered across the area in the model simulation rather than organized into an arch-like band, as clearly delineated by the AMSR-E

observation. A cloud deck covering the Tibetan Plateau discernible in the AMSR-E and MODIS observations is reasonably well reproduced by the model simulation. These similarities and discrepancies are also readily identified in a vertical cross section of the observed and simulated CloudSat radar echoes.

The examples shown in Figs. 2 and 3 imply that the SDSU, or any satellite simulator applicable to a variety of sensors with different spectral ranges, is expected to be a powerful diagnostic tool to study the three-dimensional structure of cloud systems in depth. Potential applications of the SDSU are next summarized.

#### **APPLICATION 1: MODEL EVALUATION.**

A primary application of the SDSU is to diagnose the performance of CRMs in comparison with satellite-observed radiances and backscattered electromagnetic echoes. Model evaluation studies with a satellite simulator have an advantage over the more traditional approach based on satellite retrievals (e.g., comparing surface rain rates). This is because, as depicted in Fig. 4, a satellite retrieval algorithm is an inverse model—that is, satellite measurements are inverted to find consistent input to the radiative transfer problem, based upon a number of assumptions with their characteristic underlying uncertainties. A major source of uncertainty for cloud and/or precipitation retrieval is the hydrometeor PSD. CRM simulations rarely agree with any satellite data product even if applied to the same precipitation event as observed, since the conventional PSD assumptions in retrieval algorithms generally have different historical roots from the assumptions underlying current CRM microphysical schemes. Besides the PSD, radiative emission from the surface and atmospheric gases can be an additional source of uncertainty if not properly modeled in the satellite retrieval algorithm.

These difficulties are avoided when the CRM is evaluated not with a satellite-based external data product but in terms of direct measurables such as radiances. The radiance-based model evaluation only needs a satellite simulator or a forward model to compute synthetic measurements (Fig. 4), requiring no inverse model to be invoked. While the PSD assumptions and other implicit assumptions that are built into retrieval algorithms are generally not perfectly consistent with the CRM physics, the surface and atmospheric parameters, including the PSD, are fully under the control of users of the SDSU. The SDSU user can specify the surface and/or atmospheric characterizations exactly as given by the CRM output,

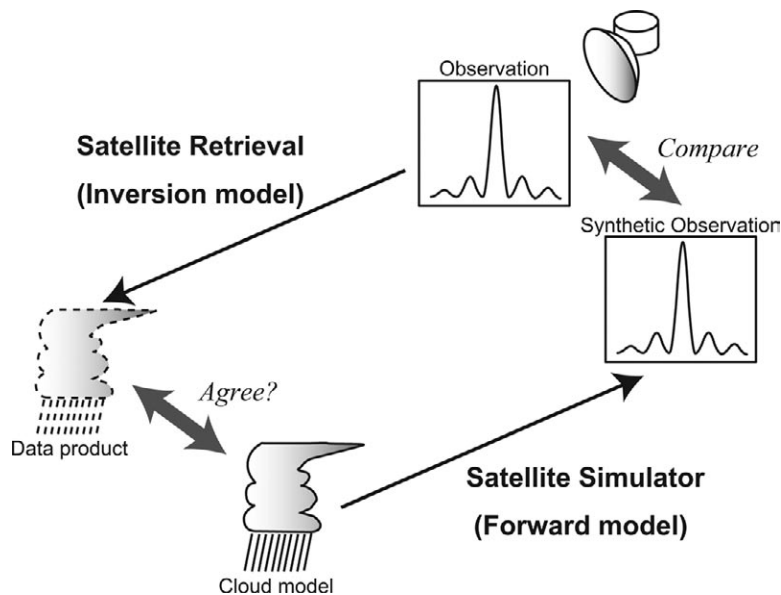


**FIG. 4. Schematic that illustrates the roles of a satellite simulator and a retrieval algorithm. A satellite simulator is a forward model in which synthetic measurements are obtained uniquely from the radiative transfer equation once all the required inputs are provided. On the other hand, a satellite retrieval algorithm is an inversion model, where the solution is retrieved by finding the input to the radiative transfer model that is compatible with a given set of measurements. Since satellite remote sensing generally involves underconstrained inversion problems, a retrieval algorithm is built on internal error models that characterize the uncertainties associated with the unmeasurables (and statistical noise associated with the measurables as well). The unmeasurables, in contrast, are controllable parameters for satellite simulators. The retrieval algorithm output (or data product) would agree with the simulator input (or cloud model) only when the error models are defined in a physically consistent manner between the satellite algorithm and simulator.**

or make a modification for testing the model sensitivity to the internal physics such as the microphysical scheme. As such, satellite simulators offer a useful testbed to validate CRM performance.

By combining data from multiple satellite instruments, the applicability of satellite simulators for evaluating CRM performance is greatly expanded, as illustrated by some recent studies, as follows. Model biases in macrophysical and microphysical quantities may be separately identified when the TRMM PR and CloudSat CPR are combined, exploiting the difference in the radar sensitivity to particle size between different microwave frequencies (Masunaga et al. 2008). Papers by Matsui et al. and Li et al. show that the combination of microwave and infrared brightness temperatures, together with radar reflectivities, provides a good test of CRM reproducibility in the

simulation of tropical convective clouds. Han et al. apply a similar technique utilizing TRMM PR and TMI data to a cold-frontal rainband simulation.

**APPLICATION 2: ALGORITHM DEVELOPMENT.** The usefulness of satellite simulators is not limited to model evaluation. The SDSU can serve as a tool to support retrieval algorithm development for current and future multisensor satellite programs. Such algorithms have combined use of passive and active microwave instruments to derive precipitation profiles, passive microwave and visible/infrared sensors to detect drizzle in maritime low clouds, and millimeter-wave radar and visible imagery to determine cloud microphysical properties.

While inversion schemes vary from one algorithm to another, typical modern satellite algorithms involve forward radiative transfer simulations to create a database or lookup table for the algorithm to search for the solution (or an ensemble of solutions). Alternatively, an inverse model may be designed using a set of forward radiative transfer simulations to train a neural network that establishes the connection between the measurements and solutions. As such, satellite

simulators can act as a forward model engine at work in the processes of constructing satellite algorithms. The core of the SDSU is indeed a collection of routines that were originally constructed for algorithm development purposes. A database of candidate solutions and neural networks are efficient and generally useful, but are based only on a finite number of forward simulations performed offline. The anticipated advance of computer capabilities could allow a forward radiative transfer model to be run online within satellite algorithms. The direct implementation of a forward model also facilitates numerical weather prediction schemes that assimilate satellite radiance data.

Another application of the SDSU is to assist in algorithm development by creating synthetic satellite observations used for testing algorithm performance. Figure 4 may also be viewed as a schematic illustrating



the potential role of satellite simulators as a testbed for satellite algorithms. Satellite simulators are particularly helpful for prospective satellite projects that involve new instrumental technologies unavailable at present, for which synthetic observations provide the unique opportunity to test the retrieval algorithm with virtual data.

**FUTURE IMPROVEMENTS.** The SDSU will be kept updated in an effort to meet the requests of users, fix bugs, and improve utility. An important upgrade being planned on a long-term basis is the implementation of more realistic hydrometeor radiative properties for frozen particles, including the effects of particle nonsphericity and inhomogeneity. Currently in the SDSU, the radiative properties such as the extinction and scattering coefficients are based on Mie solutions, for which all particles are assumed to be spherical. In reality, while cloud droplets and raindrops can be thought of as homogeneous liquid water spheres to a reasonable extent, frozen hydrometeors such as cloud ice crystals and snowflakes have highly complicated crystal structures varying dramatically with a number of factors, including ambient temperature and humidity. It is almost impossible to establish a single tractable theoretical framework applicable to arbitrarily shaped ice particles, but there are practical strategies using different approximations to model the radiative properties of inhomogeneous, nonspherical particles. In a future version of the SDSU, the present Mie LUTs will be replaced with a more realistic database of the radiative properties for frozen hydrometeors.

Another long-term plan for the upgrade is to expand the SDSU to include additional satellite sensors. The constant refrain from existing users is a request to add a lidar simulator to the SDSU. The CALIPSO lidar, when combined with other A-Train instruments such as the CloudSat CPR, has proven its capability for measuring the vertical structure of ice-cloud microphysical properties that were previously undetectable from satellites. It is expected that research interest in lidar, utilized as a component of multisensor spaceborne observatories, will continue to grow. This interest will be stimulated by the planned EarthCARE mission, which will include a lidar as part of a suite of satellite instruments.

SDSU users are encouraged to modify the distributed source code, written in the standard Fortran 90 format, and to implement new subroutines for their own research purposes if necessary. A notable example is the “spin off” Goddard SDSU being developed at

NASA GSFC. In addition to the existing three simulator components of the SDSU, lidar and broadband radiometer simulator components have been included in the Goddard version. These new instrument simulators, utilized in combination with the visible/infrared simulator, enhance the SDSU capability for analyzing aerosols as well as clouds and precipitation. The Goddard SDSU’s core interface has been reinvented 1) to include parallel computational capability, and 2) to support the NASA multiscale modeling system. With these additional features, the applicability of the Goddard SDSU is extended to support NASA’s wide variety of ongoing and planned satellite missions, including TRMM, Terra, A-Train, GPM, and possible future missions under study, such as ACE.

**DOWNLOAD THE SDSU.** The SDSU package is available for download from <http://precip.hyarc.nagoya-u.ac.jp/sdsu/index.html> for registered users. Registrants are requested to provide their name and e-mail address so that they will be notified of major upgrades. The SDSU package consists of source codes for the simulator components, Mie LUT generator with sample pre-computed LUTs, and all ancillary routines required to run the SDSU. Sample CRM inputs as demonstrated by Fig. 2 are optionally available. The SDSU User’s Guide provides comprehensive instructions for users and is available in the PDF format from the Web site above.

#### APPENDIX: GLOSSARY

ACE	Aerosol-Cloud-Ecosystems
AMSR-E	Advanced Microwave Scanning Radiometer for EOS
CALIPSO	Cloud-Aerosol Lidar and Infrared Pathfinder Satellite Observation
CERES	Clouds and the Earth’s Radiant Energy System
CFMIP	Cloud Feedback Model Intercomparison Project
COSP	CFMIP Observational Simulator Package
CPR	Cloud Profiling Radar
DPR	Dual-frequency Precipitation Radar
CRM	Cloud-resolving model
CRTM	Community Radiative Transfer Model
EarthCARE	Earth Clouds, Aerosols, and Radiation Explorer
ECSIM	EarthCARE Simulator
EOS	Earth Observing System
GCE	Goddard Cumulus Ensemble model
GSFC	Goddard Space Flight Center

GMI	GPM Microwave Imager
GPM	Global Precipitation Measurement
ISCCP	International Satellite Cloud Climatology Project
ISSARS	Instrument Simulator Suite for Atmospheric Remote Sensing
LUT	Lookup table
MODIS	Moderate Resolution Imaging Spectroradiometer
MSI	MultiSpectral Imager
NASA	National Aeronautics and Space Administration
NCEP	National Centers for Environmental Prediction
PR	Precipitation Radar
PSD	Particle size distribution
RTTOV	Radiative Transfer model for the TIROS Operational Vertical Sounder
SDSU	Satellite Data Simulator Unit
TIROS	Television Infrared Observation Satellite
TMI	TRMM Microwave Imager
TRMM	Tropical Rainfall Measuring Mission
VIRS	Visible/Infrared Scanner
WRF	Weather Research and Forecasting model

## FOR FURTHER READING

- Austin, R., and G. L. Stephens, 2001: Retrieval of stratus cloud microphysical parameters using millimeter-wave radar and visible optical depth in preparation for CloudSat. *J. Geophys. Res.*, **106**, 28 233–28 242.
- Bauer, P., E. Moreau, F. Chevallier, and U. O’Keefe, 2006: Multiple-scattering microwave radiative transfer for data assimilation applications. *Quart. J. Roy. Meteor. Soc.*, **132**, 1259–1281.
- Greco, M., W. S. Olson, and E. N. Anagnostou, 2004: Retrieval of precipitation profiles from multiresolution, multifrequency active and passive microwave observations. *J. Appl. Meteor.*, **43**, 562–575.
- Haddad, Z. S., E. A. Smith, C. D. Kummerow, T. Iguchi, M. R. Farrar, S. L. Durden, and M. Alves, 1997: The TRMM ‘day-1’ radar/radiometer combined rain-profiling algorithm. *J. Meteor. Soc. Japan*, **75**, 799–809.
- Han, M., S. Braun, W. S. Olson, P. O. G. Persson, and J.-W. Bao, 2010: Application of TRMM PR and TMI measurements to assess cloud microphysical schemes in the MM5 model for a winter storm. *J. Appl. Meteor. Climatol.*, **49**, 1129–1148.
- Kummerow, C. D., 1993: On the accuracy of the Eddington approximation for radiative transfer in the microwave frequencies. *J. Geophys. Res.*, **98**, 2757–2765.
- Li, X., W.-K. Tao, T. Matsui, C. Liu, and H. Masunaga, 2010: Improving a spectral bin microphysical scheme using TRMM satellite observations. *Quart. J. Roy. Meteor. Soc.*, **136**, 382–399.
- Masunaga, H., and C. D. Kummerow, 2005: Combined radar and radiometer analysis of precipitation profiles for a parametric retrieval algorithm. *J. Atmos. Oceanic Technol.*, **22**, 909–929.
- , T. Iguchi, R. Oki, and M. Kachi, 2002a: Comparison of rainfall products derived from TRMM Microwave Imager and Precipitation Radar. *J. Appl. Meteor.*, **41**, 849–862.
- , T. Y. Nakajima, T. Nakajima, M. Kachi, R. Oki, and S. Kuroda, 2002b: Physical properties of maritime low clouds as retrieved by combined use of Tropical Rainfall Measuring Mission Microwave Imager and Visible/Infrared Scanner: Algorithm. *J. Geophys. Res.*, **107**, doi:10.1029/2001JD000743.
- , M. Satoh, and H. Miura, 2008: A joint satellite and global cloud-resolving model analysis of a Madden-Julian Oscillation event: Model diagnosis. *J. Geophys. Res.*, **113**, D17210, doi:10.1029/2008JD009986.
- Matricardi, M., F. Chevallier, G. Kelly, and J.-N. Thépaut, 2004: An improved general fast radiative transfer model for the assimilation of radiance observations. *Quart. J. Roy. Meteor. Soc.*, **130**, 153–173.
- Matsui, T., X. Zeng, W.-K. Tao, H. Masunaga, W. S. Olson, and S. Lang, 2009: Evaluation of long-term cloud-resolving model simulations using satellite radiance observations and multifrequency satellite simulators. *J. Atmos. Oceanic Technol.*, **26**, 1261–1274.
- Nakajima, T. Y., H. Murakami, M. Hori, T. Nakajima, T. Aoki, T. Oishi, and A. Tanaka, 2003: Efficient use of an improved radiative transfer code to simulate near-global distributions of satellite-measured radiances. *Appl. Optics*, **42**, 3460–3471.
- Shao, H. and G. Liu, 2004: Detecting drizzle in marine warm clouds using combined visible, infrared and microwave satellite data. *J. Geophys. Res.*, **109**, D07205.
- Tanelli, S., 2009: Development of NASA’s integrated instrument simulator suite for atmospheric remote sensing. 34th AMS Conference on Radar Meteorology, Williamsburg, VA, Amer. Meteor. Soc.
- Tao, W.-K., and Coauthors, 2009: Goddard multi-scale modeling systems with unified physics. *Annales Geophys.*, **27**, 3055–3064.
- Voors, R., and Coauthors, 2007: ECSIM: the simulator framework for EarthCARE. *Proc. SPIE*, **6744**, 67441Y, doi:10.1117/12.737738.